Power efficiency of Hall-like devices: Comparison between reciprocal and antireciprocal Onsager relations

Jean-Eric Wegrowe, Luqian Zhou, Sariah Al Saati

▶ **To cite this version:**

Jean-Eric Wegrowe, Luqian Zhou, Sariah Al Saati. Power efficiency of Hall-like devices: Comparison between reciprocal and antireciprocal Onsager relations. Physical Review B, 2024, 110 (2), pp.024412. ⟨10.1103/PhysRevB.110.024412⟩. ⟨hal-04838302⟩

HAL Id: hal-04838302

https://hal.science/hal-04838302v1

Submitted on 14 Dec 2024

HAL is a multi-disciplinary open access archive for the deposit and dissemination of scientific research documents, whether they are published or not. The documents may come from teaching and research institutions in France or abroad, or from public or private research centers.

L'archive ouverte pluridisciplinaire **HAL**, est destinée au dépôt et à la diffusion de documents scientifiques de niveau recherche, publiés ou non, émanant des établissements d'enseignement et de recherche français ou étrangers, des laboratoires publics ou privés.

HAL Authorization

Power efficiency of Hall-like devices: Comparison between reciprocal and antireciprocal Onsager relations

Jean-Eric Wegrowe [1,*] Luqian Zhou [1] and Sariah Al Saati [2]
[1] *LSI, École Polytechnique, CEA/DRF/IRAMIS, CNRS, Institut Polytechnique de Paris, 91120 Palaiseau, France*
[2] *Centre de Physique Théorique, 91120 Palaiseau, France*

(Received 24 March 2024; revised 17 June 2024; accepted 26 June 2024; published 9 July 2024)

Two well-known Hall-like effects occur in ferromagnets: the anomalous Hall effect (AHE) and the planar Hall effect (PHE). AHE is analogous to the classical Hall effect and is characterized by the antireciprocal Onsager relation (antisymmetric conductivity matrix), whereas PHE is defined by the reciprocal Onsager relation (symmetric conductivity matrix). The distinction is fundamental, as it stems from time-reversal symmetry breaking at the microscopic scale. We examine theoretically the Hall current generated in both AHE and PHE, along with the electric power that can be transferred from the edges of the Hall bar into a load circuit. Using a variational method based on the second law of thermodynamics, we derive expressions for the distribution of the electric currents, the distribution of electric carriers, and the power efficiencies. Our results show that the distribution of the transverse Hall current is identical for both AHE and PHE (with all other parameters being equals) but the longitudinal current and the power dissipated differ at the second order in the Hall angle.

DOI: 10.1103/PhysRevB.110.024412

I. INTRODUCTION

Exactly 200 years ago, in 1824, Sadi Carnot published his seminal work that first formulated the second law of thermodynamics [1]. Independently, 55 years later, in 1879, Edwin Hall reported on the phenomenon that would come to bear his name [2]. Another 52 years later, in 1931, Lars Onsager published two papers [3,4] on the reciprocity relations describing cross effects in transport phenomena, a breakthrough that earned him the Nobel Prize in 1968 [5]. In recent years, building on these three foundational discoveries, a series of fascinating studies have been devoted to the anomalous Hall effect (AHE), and its relation with topological materials. This research began with Karplus and Luttinger's 1954 paper [6], and continued for 50 years [7–10] culminating in Haldane's influential work in 2004 [11], which contributed to his Nobel Prize in 2016. This field remains highly active today [12–15], especially within the context of new topological materials exhibiting unconventional AHE [16,17]. On the other hand, also in 1954, Golberg and Davis proposed the name of planar Hall effect (PHE) [18], while generalizing the description of the ordinary Hall effect to an arbitrary direction of the magnetic field. The PHE then simply appears as a supplementary contribution to the voltage measured in the Hall configuration, generated by the same effective magnetic field that produces AHE [19,20].

In his first paper, Onsager formulated the reciprocity relation of the first kind, known as reciprocal, based on the microscopic property of time-reversal symmetry [3]. Subsequently, his second paper addressed the reciprocity relation of the second kind, referred to as antireciprocal, which emerged from the partial breaking of this time-reversal symmetry [4]. The first reciprocal relation leads to a symmetric matrix of the transport coefficients, while the second antireciprocal relation leads to an antisymmetric transport matrix. Because of his simplicity, seniority [6,18], and ubiquity [21,22], PHE and AHE effects can be considered as archetype, that allow us to compare the dissipative properties of reciprocal vs nonreciprocal Onsager relations.

More precisely, in the case of ordinary electric transport in ferromagnetic conductors, the effective magnetic field is responsible for *two modifications* of the symmetry of the out-of-equilibrium system. First, it breaks the initial isotropy of the conductivity with imposing axial symmetry (along the effective field), defining both the anisotropic magnetoresistance and the PHE. Second, it breaks the time-invariance symmetry, defining Hall effect (or AHE) with the introduction of the antireciprocal Onsager cross coefficient. In both cases, the off-diagonal coefficients induce a coupling between the two directions x and y in the plane of the Hall device. Consequently, PHE and AHE define two fundamentally different ways to inject a lateral current from the edges of the Hall bar into a lateral load circuit. It is worth noting that in ferromagnets or ferrimagnets (or some unconventional magnets), the lateral Hall current produced by AHE or PHE is spin polarized, enabling its use in switching an adjacent ferromagnetic layer [23], an effect known as spin-orbit torque [24]. However, in the present report, the spin degrees of freedom are not considered, indicating that the load circuit is positioned at significant distance from the edges of the Hall bar, typically beyond the nanometric scale.

The question treated in this work is to understand why and how the two Hall currents injected respectively with PHE and AHE are of "different nature" from the point of view of the dissipation. In order to answer to this question, we perform a comparative study—with a synoptic presentation—of both

*Contact author: jean-eric.wegrowe@polytechnique.edu

 ©2024 American Physical Society

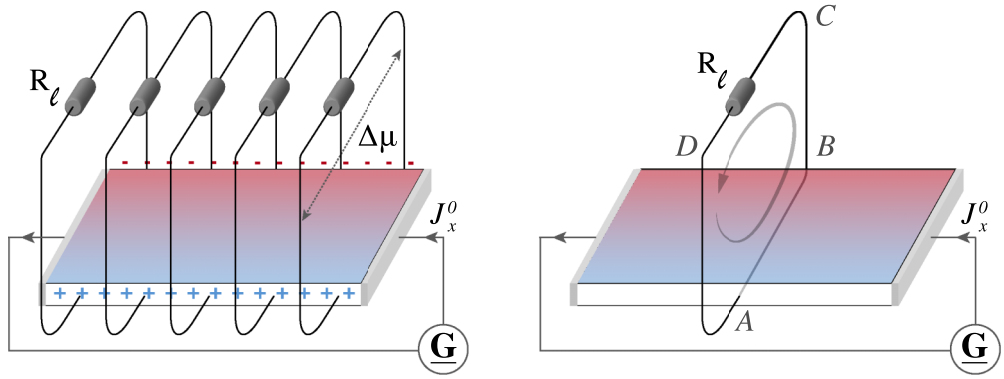

FIG. 1. Left: illustration of a Hall bar connected to a load circuit with resistance R_ℓ maintaining translation invariance along the x direction. The sign of the electric-charge accumulation is indicated by red (-) and blue (+) colors (see the calculated profile in Fig. 3). Right: Integration loop ABCDA defined on one of the yz vertical planes. A magnetic vector $\vec{m}$ is present but it is not represented in the picture.

kinds of transverse current produced at the stationary state inside the magnetic material, and injected into the load circuit, all other parameters being equal.

The analysis primarily relies on a variational method based on the second law of thermodynamics, following a methodology established in a series of prior publications [25–29] whose objectives were to compute the power dissipated by the Hall current in a perfect Hall bar in contact with a lead circuit. In these previous publications, it was observed that due to the small value of the Hall angle (below 1%), the properties of the dissipated power were found to be surprisingly close to what could have been expected from a standard lumped-element circuit [30,31]. The validity of the results have however been confirmed in preliminary experiments performed on the AHE in GdCo ferrimagnets [32].

II. MODEL

The system we consider consists of a thin, homogeneous, magnetized conducting layer with length L and width ℓ, connected to an electric generator as depicted in Fig. 1. The material used can be a conducting ferromagnet, antiferromagnet, altermagnet, or any kind of conducting materials that can be described with a single effective magnetic field, or effective axial vector $\vec{m}$ (responsible for both AHE and PHE). We assume that the conducting layer is planar, invariant by translation along the x axis $\ell \ll L$ (this excludes the region in contact with the power generator). We omit any component of the electric current along the z axis, and we consider that the two lateral edges are symmetric.

We define the distribution of electric charge carriers by $n(y) = n_0 + \delta n(y)$, where $\delta n(y)$ is the charge accumulation and n_0 the homogeneous density in the electrically neutral system. Due to the symmetry of the device and global charge conservation we have $\int_{-\ell}^{+\ell} \delta n\, dy = 0$, and the total charge-carrier density is constant $n_{\rm tot} = \frac{1}{2\ell}\int n\, dy$. For the sake of simplicity, we assume a global charge neutrality so that $n_{\rm tot} = n_0$. Additionally, the external generator injects a current along the x direction, meaning that the global current flowing in the x direction throughout the device is also constant along x, by definition of the galvanostatic condition. This is expressed as $\int_{-\ell}^{\ell} J_x(y)dy = 2\ell J_x^0$.

Furthermore, in Sec. V, we will consider the case where a Hall current is injected into the load circuit contacted at the lateral edges. We must then introduce the Joule dissipation due to the load resistance. Unlike for the x direction, there is no external generator in the y direction, so that the loop integral of current in the $\{yz\}$ plane vanishes : $\oint_{ABCDA} Jdl = 0$, where the integration path $ABCD$ is sketched in Fig. 1(b). This can be equivalently written $\int_{AB} Jdl + \int_{BCDA} Jdl = \int_{-\ell}^{\ell} J_y(y)dy + \int_{BCDA} Jdl = 0$. The definite integral $\int_{BCDA} Jdl$ is a constant that we do not know at the moment, and we will represent the constant as $\int_{BCDA} Jdl = -2lJ_y^0$, where J_y^0 is determined in Sec. V. In summary, we can write the global constraint on the y direction as $\int_{-\ell}^{\ell} J_y(y)dy = 2lJ_y^0$.

III. JOULE DISSIPATION INCLUDING SCREENING

The charge accumulation is governed by Poisson's equation $\nabla^2 V = -\frac{q}{\varepsilon}\delta n$, where V is the electrostatic potential, q is the electric charge, and ε is the electric permittivity. The local electrochemical potential $\mu(x, y)$—that takes into account not only the electrostatic potential V but also the energy (or the entropy) responsible for the diffusion—is given by the expression [33,34] (local equilibrium is assumed everywhere)

$$\mu = \frac{kT}{q}\ln\left(\frac{n}{n_0}\right) + V, \tag{1}$$

where k is the Boltzmann constant and the temperature T is the temperature of the heat bath in the case of a nondegenerate semiconductor, or the Fermi temperature T_F in the case of a fully degenerate conductor [35]. Poisson's equation now reads

$$\nabla^2\mu - \lambda_D^2\frac{q}{\varepsilon}n_0\nabla^2\ln\left(\frac{n}{n_0}\right) + \frac{q}{\varepsilon}\delta n = 0, \tag{2}$$

where $\lambda_D = \sqrt{\frac{kT\varepsilon}{q^2 n_0}}$ is the Debye-Fermi length (T is the temperature and k the Boltzmann constant). On the other hand, the transport equation under a magnetic field is given by Ohm's law:

$$\vec{J} = -\hat{\sigma}\vec{\nabla}\mu = -qn\hat{\eta}\vec{\nabla}\mu, \tag{3}$$

where the transport coefficients are the conductivity tensor $\hat{\sigma}$ or the mobility tensor $\hat{\eta}$.

Based on the uniaxial symmetry imposed by the effective magnetic field (where the resistivity along the effective magnetic field differs from that within the plane) and the antireciprocal symmetry due to the same effective magnetic field, Ohm's law for resistivity takes the form[18,36–38]

$$\vec{\mathcal{E}} = \rho\vec{J} + \Delta\rho(\vec{m}\cdot\vec{J})\vec{m} + \rho_H\,\vec{m}\times\vec{J}, \tag{4}$$

where we have introduced the resistivity of the isotropic material ρ, the anisotropic magnetoresistance $\Delta\rho/\rho$, and the Hall resistivity ρ_H. The resistivity matrix is deduced from Eq.(4):

$$\hat{\rho} = \begin{pmatrix} \rho+\Delta\rho m_x^2 & \Delta\rho m_x m_y - \rho_H m_z & \Delta\rho m_x m_z + \rho_H m_y \\ \Delta\rho m_y m_x + \rho_H m_z & \rho+\Delta\rho m_y^2 & \Delta\rho m_y m_z - \rho_H m_x \\ \Delta\rho m_z m_x - \rho_H m_y & \Delta\rho m_z m_y + \rho_H m_x & \rho+\Delta\rho m_z^2 \end{pmatrix}, \tag{5}$$

where the unit vector $\vec{m}$ gives the direction of the magnetization with respect to the orthogonal basis attached to the Hall bar. The unit vector $\vec{m}$ can be expressed as a function of the radial angle θ and the orthoradial angle φ, such that $m_x = \sin(\theta)\,\cos(\varphi)$, $m_y = \sin(\theta)\,\sin(\varphi)$, $m_z = \cos\theta$. In order to compare the planar Hall effect with the anomalous Hall effect, we choose the material of the Hall bar such that $\rho \gg \Delta\rho \gg \rho_H$ for the planar Hall effect (this is typically the case for NiFe alloys [39]) and $\rho \gg \rho_H \gg \Delta\rho$ for the anomalous Hall effect (this is typically the case for GdCo alloys [32,39]). In the following, the index *pl* stands for PHE (left column below) and the index *an* stands for AHE (right column below). In addition, we only consider an electric current flowing inside the *xy* plane, thus the matrix Eq. (5) can be reduced to 2×2 matrices:

$$\hat{\rho}_{pl} = \begin{pmatrix} \rho & \Delta\rho\, m_x m_y \\ \Delta\rho\, m_y m_x & \rho \end{pmatrix} \quad\text{and}\quad \hat{\rho}_{an} = \begin{pmatrix} \rho & -\rho_H\, m_z \\ \rho_H\, m_z & \rho \end{pmatrix}. \tag{6}$$

We then define the ratio of the off-diagonal coefficient over the diagonal coefficient:

$$\Theta_{pl} = \frac{\Delta\rho}{\rho}\,\sin^2(\theta)\,\sin(2\varphi) \quad\text{and}\quad \Theta_{an} = -\frac{\rho_H}{\rho}\,\cos(\theta). \tag{7}$$

The angular dependence of the parameters defined in Eqs. (6) and (7) influences the Hall voltage by charge accumulation at the edges, and is an unambiguous signature for the distinction between AHE and PHE [32,39]. However, in our context (theory and experiment), we will choose the magnetization direction such that $\theta = \pi/2$ and $\varphi = -\pi/4$ for the PHE and $\theta = 0$ for AHE. We will also consider two materials such that $\Delta\rho/\rho \approx \rho_H/\rho$ in order to have $\Theta = \Theta_{an} = -\Theta_{pl}$. Furthermore, since $\Delta\rho/\rho$ and ρ_H/ρ are of the order of 1% maximum, we have $\sin(\Theta) \approx \Theta$ and we will call Θ the "Hall angle."

The conductivity matrix can be computed as the inverse of the resistivity matrix $\hat{\sigma} = \hat{\rho}^{-1}$ which allows us to compute the mobility tensor $\hat{\sigma} = qn\hat{\eta}$:

$$\hat{\eta}_{pl} = \begin{pmatrix} \eta & \eta_{pl} \\ \eta_{pl} & \eta \end{pmatrix} = \eta\begin{pmatrix} 1 & -\Theta \\ -\Theta & 1 \end{pmatrix} \quad\text{and}\quad \hat{\eta}_{an} = \begin{pmatrix} \eta & \eta_{an} \\ -\eta_{an} & \eta \end{pmatrix} = \eta\begin{pmatrix} 1 & \Theta \\ -\Theta & 1 \end{pmatrix}. \tag{8}$$

We can then express the Joule dissipation density in terms of the current vector components J_x, J_y:

$$p_J = \vec{J}\cdot\vec{\nabla}\mu. \tag{9}$$

Using Ohm's law expressed in Eq. (3), the gradients of the chemical potentials $\vec{\nabla}\mu$ read

$$\begin{aligned} \vec{\nabla}\mu^{\mathrm{pl}} &= -\frac{1}{qn}\hat{\eta}_{pl}^{-1}\vec{J} & \vec{\nabla}\mu^{\mathrm{an}} &= -\frac{1}{qn}\hat{\eta}_{an}^{-1}\vec{J} \\ &= -\frac{1}{qn\eta(1-\Theta^2)}\begin{pmatrix} 1 & \Theta \\ \Theta & 1 \end{pmatrix}\begin{pmatrix} J_x \\ J_y \end{pmatrix}, \quad\text{and} & &= -\frac{1}{qn\eta(1+\Theta^2)}\begin{pmatrix} 1 & -\Theta \\ \Theta & 1 \end{pmatrix}\begin{pmatrix} J_x \\ J_y \end{pmatrix}, \\ \vec{\nabla}\mu^{\mathrm{pl}} &= -\frac{n_0}{n\sigma_{pl}}\begin{pmatrix} J_x+\Theta J_y \\ \Theta J_x + J_y \end{pmatrix}, & \vec{\nabla}\mu^{\mathrm{an}} &= -\frac{n_0}{n\sigma_{an}}\begin{pmatrix} J_x-\Theta J_y \\ \Theta J_x + J_y \end{pmatrix}, \end{aligned} \tag{10}$$

where, for convenience, we have introduced the two constant conductivities (i.e., the bulk conductivities for $y \gg \lambda_D$)

$$\sigma_{pl} = qn_0\eta(1-\Theta^2) \qquad\text{and}\qquad \sigma_{an} = qn_0\eta(1+\Theta^2). \tag{11}$$

Since ρ is the intrinsic value of the resistivity of the material [32,39] (that does not depend on Θ) and assuming identical material for both AHE and PHE, we have $\sigma_{pl} = \frac{1}{\rho(1-\Theta^2)}$ and $\sigma_{ah} = \frac{1}{\rho(1+\Theta^2)}$ and

$$p_J^{\mathrm{pl}} = -\frac{n_0}{n\sigma_{pl}}\left(J_x^2 + J_y^2 + 2\Theta J_x J_y\right) \qquad\text{and}\qquad p_J^{\mathrm{an}} = -\frac{n_0}{n\sigma_{an}}\left(J_x^2 + J_y^2\right). \tag{12}$$

The expression of the Joule power dissipated by the system reads

$$P_J = S_{\rm lat}\int_{-\ell}^{\ell} p_J(y)dy, \tag{13}$$

which gives, respectively,

$$P_J^{\rm pl} = \frac{S_{\rm lat}}{\sigma_{pl}}\int_{-\ell}^{\ell}\frac{n_0}{n}\left(J_x^2+J_y^2+2\Theta J_xJ_y\right)dy \qquad \text{and} \qquad P_J^{\rm an} = \frac{S_{\rm lat}}{\sigma_{an}}\int_{-\ell}^{\ell}\frac{n_0}{n}\left(J_x^2+J_y^2\right)dy, \tag{14}$$

where $S_{\rm lat}$ is the lateral surface of the Hall bar (product of the length L by the thickness), and 2ℓ is the width. As expected the two expressions of the Joule heating for PHE and AHE turn out to be significantly different.

IV. CURRENTS AND CHARGE DENSITIES WITHOUT LOAD CIRCUIT

We first consider the case of the Hall bar without load circuit. The stationary state is defined by the *least dissipation principle* which states that the current is distributed so as to minimize Joule heating P_J while satisfying the given constraints [40–42]. Without load circuit, in the notations of Sec. III, the integration path ABCD is reduced to AB and the global constraint along the y direction is zero: $\int_{-\ell}^{\ell} J_y(y)dy = 0$.

The global constraints read

$$\int_{-\ell}^{\ell} n(y)dy = 2\ell n_0 \quad \text{and} \quad \int_{-\ell}^{\ell} J_x(y)dy = 2\ell J_x^0 \quad \text{and} \quad \int_{-\ell}^{\ell} J_y(y)dy = 0. \tag{15}$$

We define for convenience the reduced power $\tilde{P}_J = \frac{q\eta(1\pm\Theta^2)}{S_{\rm lat}}P_J$. Let us introduce the two Lagrange multiplayers λ_x and λ_n, corresponding to the two constraints Eqs. (15). The functional to be minimized is then given by

$$\tilde{\mathcal{P}}_J^{\rm pl} = \int_{-\ell}^{\ell}\left(\frac{J_x^2+J_y^2+2\Theta J_xJ_y}{n} - \lambda_x J_x - \lambda_y J_y - \lambda_n n\right)dy \quad \text{and} \quad \tilde{\mathcal{P}}_J^{\rm an} = \int_{-\ell}^{\ell}\left(\frac{J_x^2+J_y^2}{n} - \lambda_y J_y - \lambda_x J_x - \lambda_n n\right)dy. \tag{16}$$

The minimum corresponds to

$$\frac{\delta\tilde{\mathcal{P}}_J}{\delta J_x} = 0 \quad \text{and} \quad \frac{\delta\tilde{\mathcal{P}}_J}{\delta J_y} = 0 \quad \text{and} \quad \frac{\delta\tilde{\mathcal{P}}_J}{\delta(n)} = 0, \tag{17}$$

which give, respectively,

$$\begin{cases} 2J_x + 2\Theta J_y = n\lambda_x \\ 2J_y + 2\Theta J_x = n\lambda_y \\ J_x^2+J_y^2+2\Theta J_xJ_y = -\lambda_n n^2 \end{cases} \quad \text{and} \quad \begin{cases} 2J_x = n\lambda_x \\ 2J_y = n\lambda_y \\ J_x^2+J_y^2 = -\lambda_n n^2 \end{cases}. \tag{18}$$

By integrating the two first equations across the bar from $-l$ to l, and applying the constraints, we can explicitly solve λ_x and λ_y. Substituting these results back into the equations above, we obtain J_x and J_y as follow:

$$\begin{cases} J_x^{\rm pl}(y) = J_x^0\dfrac{n(y)}{n_0} \\ J_y^{\rm pl}(y) = 0 \end{cases} \quad \text{and} \quad \begin{cases} J_x^{\rm an}(y) = J_x^0\dfrac{n(y)}{n_0} \\ J_y^{\rm an}(y) = 0 \end{cases}. \tag{19}$$

As can be observed, the current density is not homogeneous throughout the sample [since $n(y) \neq n_0$], and it exhibits the same form for both AHE and PHE.

Then inserting the solution Eq. (19) into the transport equations Eq. (10), we deduce

$$\begin{cases} \partial_x\mu^{\rm pl}(y) = -\frac{J_x^0}{\sigma_{pl}} \\ \partial_y\mu^{\rm pl}(y) = -\frac{\Theta J_x^0}{\sigma_{pl}} \end{cases} \quad \text{and} \quad \begin{cases} \partial_x\mu^{\rm an}(y) = -\frac{J_x^0}{\sigma_{an}} \\ \partial_y\mu^{\rm an}(y) = -\frac{\Theta J_x^0}{\sigma_{an}} \end{cases}. \tag{20}$$

As a consequence, the electrochemical potential of the stationary state is harmonic in both cases: $\nabla^2\mu = 0$. Since the profile of the lateral current $J_y(y)$ is defined by the charge density $n(y)$, Poisson's equation Eq. (2) for $\nabla^2\mu = 0$ gives the equation

$$\lambda_D^2\partial_y^2\ln\left(1+\frac{\delta n}{n_0}\right) = \frac{\delta n}{n_0}. \tag{21}$$

Assuming $\delta n \ll n_0$, we have, at the first order

$$\lambda_D^2\partial_y^2\left(\frac{\delta n}{n_0}\right) = \frac{\delta n}{n_0}, \tag{22}$$

which gives us

$$\frac{\delta n(y)}{n_0} = A\,\mathrm{ch}(y/\lambda_D) + B\,\mathrm{sh}(y/\lambda_D). \tag{23}$$

Once again, the boundary conditions for the density n are not defined locally but globally by Eq. (15). We can specify the boundary conditions for $\partial_y \frac{\delta n(y)}{n_0}$ noting that for the stationary solutions of Eq. (19) for both systems gives us

$$E_y = -\partial_y V \tag{24}$$

$$= -\partial_y \mu + \frac{kT}{q}\partial_y\left(\frac{\delta n}{n_0}\right), \tag{25}$$

$$E_y = -\frac{\Theta J_x^0}{\sigma_h} + \frac{kT}{q}\partial_y\left(\frac{\delta n}{n_0}\right), \tag{26}$$

where σ_h is given by σ_{pl} or σ_{an}.

We specify these conditions at the edges of the sample for $E_y(\pm\ell) = E_y(\pm\infty)$, which correspond to the electric field at the exterior of the bar, assuming that the bar is surrounded by vacuum. If we define $2\Delta^{\pm}E_\infty = E_y(\infty) \pm E_y(-\infty)$, then the approximated solution of δn is given for both cases by

$$\frac{q\lambda_D}{\varepsilon}\delta n(y) = \Delta^- E_\infty \frac{\mathrm{ch}(y/\lambda_D)}{\mathrm{sh}(l/\lambda_D)} + \left(\Delta^+ E_\infty + \frac{\Theta J_x^0}{\sigma_h}\right)\frac{\mathrm{sh}(\mathrm{y}/\lambda_\mathrm{D})}{\mathrm{ch}(\mathrm{l}/\lambda_\mathrm{D})}, \tag{27}$$

where σ_h is here again given by σ_{pl} or σ_{an}.

As can be seen, the the profiles of the screening are similar for both AHE and PHE in the perfect Hall-like device. A difference can be seen (at the second order in Θ) in terms of the conductivities σ_{pl} and σ_{an} given in Eq. (11).

V. CURRENT INJECTION IN THE LOAD CIRCUIT

The solution found in the preceding section is valid as long as the dissipation due to charge leakage at the edges is negligible compared to the dissipation inside the device. However, if it is no longer the case, the stationary regime should be reconsidered by introducing the dissipation due to the resistance of a lateral load circuit that connects the edges of the Hall bar. To account for this additional dissipation, we introduce the load resistivity R_ℓ ($\Omega \cdot \mathrm{m}^2$) of the lateral circuit. The power dissipated in the lateral circuit is

$$P_{\mathrm{lat}} = \frac{S_{\mathrm{lat}}\,\Delta\mu^2}{R_\ell},$$

where $\Delta\mu = \mu(+\ell) - \mu(-\ell)$ is the difference in the chemical potential between both edges. Note that due to our assumption of the invariance along x, we do not address the scenario where a resistance is connected to the two edges of the Hall bar with two contacts located at a given position somewhere in the bar. Indeed, such a contact would break the translation invariance symmetry along x, and would distort the current lines in a manner determined by the contact's geometry and resistivity details. This contact-specific effect is not relevant in the context of this study. Instead, the relevant contact we consider is sketched in Fig. 1 (left). It is an ideal version of the "perfect Hall bar," which can nevertheless be approximated experimentally [32,39]. Incidentally, it is understood that the primary advantage of the Corbino disk over Hall-bar devices lies in its easier design of two quasiperfect concentric equipotentials with circular symmetry as opposed to two nearly perfect longitudinal equipotentials with translation symmetry.

A. Stationary currents

The difference of chemical potential can be expressed as a function of the current:

$$\Delta\mu^{\mathrm{pl}} = \int_{-\ell}^{+\ell} dy\,\partial_y\mu = -\int_{-\ell}^{+\ell} dy\,\frac{J_y + \Theta J_x}{qn\eta(1-\Theta^2)} \quad \text{and} \quad \Delta\mu^{\mathrm{an}} = \int_{-\ell}^{+\ell} dy\,\partial_y\mu = -\int_{-\ell}^{+\ell} dy\,\frac{J_y + \Theta J_x}{qn\eta(1+\Theta^2)}, \tag{28}$$

so that

$$P_{\mathrm{lat}}^{\mathrm{pl}} = \frac{S_{\mathrm{lat}}}{R_\ell (q\eta)^2(1-\Theta^2)^2}\left(\int_{-\ell}^{+\ell} dy \frac{J_y + \Theta J_x}{n}\right)^2 \quad \text{and} \quad P_{\mathrm{lat}}^{\mathrm{an}} = \frac{S_{\mathrm{lat}}}{R_\ell (q\eta)^2(1+\Theta^2)^2}\left(\int_{-\ell}^{+\ell} dy \frac{J_y + \Theta J_x}{n}\right)^2. \tag{29}$$

As in the preceding section, we define the reduced power $\tilde{P} = \frac{q\eta(1\pm\Theta^2)}{S_{\mathrm{lat}}}P$. The total power dissipated is then

$$\tilde{P}^{\mathrm{pl}} = \tilde{P}_J + \tilde{P}_{\mathrm{lat}} = \int_{-\ell}^{+\ell} dy \frac{J_x^2 + J_y^2 + 2\Theta J_x J_y}{n} + \alpha^{\mathrm{pl}}\frac{2l}{n_0}\left(\frac{n_0}{2\ell}\int_{-\ell}^{+\ell} dy \frac{J_y + \Theta J_x}{n}\right)^2 \quad \text{and} \quad \tilde{P}^{\mathrm{an}} = \tilde{P}_J + \tilde{P}_{\mathrm{lat}} = \int_{-\ell}^{+\ell} dy \frac{J_x^2 + J_y^2}{n} + \alpha^{\mathrm{an}}\frac{2l}{n_0}\left(\frac{n_0}{2\ell}\int_{-\ell}^{+\ell} dy \frac{J_y + \Theta J_x}{n}\right)^2, \tag{30}$$

where we have introduced the dimensionless control parameter $\alpha^h = \frac{2\ell}{R_\ell \sigma_h}$.

Note that this control parameter α is defined by the ratio $\alpha = \frac{R}{R_\ell}$ of the resistance of the material $R \equiv \frac{V}{J_x^0} = \frac{2\ell}{\sigma_h}$ over the load resistance R_ℓ [32]. The case $\alpha \to 0$ corresponds to perfect Hall bar while the case $\alpha \to \infty$ corresponds to the perfect Corbino disk [25,39]. The exponent of index h denotes, respectively, $h = pl$ for the planar Hall system and $h = an$ for the anomalous

Hall system. We define for convenience the constant A^h:

$$A^h \equiv \frac{n_0}{2\ell}\int_{\ell}^{\ell}\frac{\Theta J_x + J_y}{n}dy. \tag{31}$$

At this stage, we can adopt the constraint on $J_y(y)$ as discussed in the section above:

$$\int_{-\ell}^{\ell} J_y(y)dy = 2\ell J_y^{0,h}, \tag{32}$$

where $J_y^{0,h}$ is some constant for each system which will be determined later.

The minimization of the corresponding functional $\tilde{\mathcal{P}}$ now reads

$$\begin{aligned} \alpha^{\rm pl}A^{\rm pl}\Theta + J_x + \Theta J_y &= \frac{\lambda_x n}{2}, \\ \alpha^{\rm pl}A^{\rm pl} + J_y + \Theta J_x &= \frac{\lambda_y n}{2}, \end{aligned} \quad \text{and} \quad \begin{aligned} \alpha^{\rm an}A^{\rm an}\Theta + J_x &= \frac{\lambda_x n}{2}, \\ \alpha^{\rm an}A^{\rm an} + J_y &= \frac{\lambda_y n}{2}. \end{aligned} \tag{33}$$

Once again, applying the global constraints given by Eqs. (15) along with the third replaced by Eq. (32), we can immediately solve from these two equations

$$\begin{aligned} \lambda_x &= \frac{2}{n_0}\left(\alpha^{\rm pl}A^{\rm pl}\Theta + J_x^0 + \Theta J_y^{0,pl}\right), \\ \lambda_y &= \frac{2}{n_0}\left(\alpha^{\rm pl}A^{\rm pl} + \Theta J_x^0 + J_y^{0,pl}\right), \end{aligned} \quad \text{and} \quad \begin{aligned} \lambda_x &= \frac{2}{n_0}\left(\alpha^{\rm an}A^{\rm an}\Theta + J_x^0\right), \\ \lambda_y &= \frac{2}{n_0}\left(\alpha^{\rm an}A^{\rm an} + J_y^{0,an}\right). \end{aligned} \tag{34}$$

Substituting these solutions back to the equations, we get

$$\begin{aligned} J_x &= \frac{n}{n_0}J_x^0, \\ J_y &= \frac{n}{n_0}J_y^{0,pl} + \alpha^{\rm pl}A^{\rm pl}\left(\frac{n}{n_0}-1\right), \end{aligned} \quad \text{and} \quad \begin{aligned} J_x &= \frac{n}{n_0}J_x^0 + \alpha^{\rm an}A^{\rm an}\Theta\left(\frac{n}{n_0}-1\right), \\ J_y &= \frac{n}{n_0}J_y^{0,an} + \alpha^{\rm an}A^{\rm an}\left(\frac{n}{n_0}-1\right). \end{aligned} \tag{35}$$

For simplicity, we focus on a system which obeys the local conservation of electric charges $\nabla\cdot\mathbf{J}=0$, which leads to $\frac{\partial J_x}{\partial x} + \frac{\partial J_y}{\partial y} = 0$. Since the system is invariant along the x direction, we have $\frac{\partial J_x}{\partial x} = 0$. Then this will lead to the result that $\frac{\partial J_y}{\partial y} = 0$. Thus, this requires that coefficient in factor of $n(y)$ vanishes, which leads to $J_y^0 = -\alpha A$. We get, eventually,

$$\begin{aligned} J_x &= \frac{n}{n_0}J_x^0, \\ J_y &= J_y^{0,pl}, \end{aligned} \quad \text{and} \quad \begin{aligned} J_x &= \frac{n}{n_0}J_x^0 - J_y^{0,an}\Theta\left(\frac{n}{n_0}-1\right), \\ J_y &= J_y^{0,an}. \end{aligned} \tag{36}$$

Substituting these solutions back to the definition of $A^{pl/an}$ given by Eq. (31), we obtain the following equation

$$J_y^{0,pl}\left(1+\alpha\int\frac{n_0}{n}\frac{dy}{2\ell}\right) = -\alpha\Theta J_x^0 \quad \text{and} \quad J_y^{0,an}\left(1+\alpha\Theta^2+\alpha(1-\Theta^2)\int\frac{n_0}{n}\frac{dy}{2\ell}\right) = -\alpha\Theta J_x^0. \tag{37}$$

Assuming that $\delta n \ll n_0$, we have *at the first order* $\frac{n_0}{2\ell}\int_{-\ell}^{+\ell}\frac{dy}{n(y)} \simeq 1$, thus we can solve

$$\begin{aligned} J_x &= \frac{n}{n_0}J_x^0, \\ J_y &= -\frac{\alpha}{1+\alpha}\Theta J_x^0, \end{aligned} \quad \text{and} \quad \begin{aligned} J_x &= \frac{n}{n_0}J_x^0 + \Theta^2\frac{\alpha}{1+\alpha}\left(\frac{n}{n_0}-1\right)J_x^0, \\ J_y &= -\frac{\alpha}{1+\alpha}\Theta J_x^0. \end{aligned} \tag{38}$$

The results Eqs. (38) show that, at the first order in the charge accumulation, the distributions of the transverse Hall current J_y are identical for both the AHE and the PHE, and a difference can be seen at the second order in the Hall angle Θ for the longitudinal current J_x. We conclude that the fundamental symmetry differences have been leveled out by the application of the minimum power dissipation principle derived from the second law of thermodynamics assuming comparable Hall angle Θ for AHE and PHE [i.e., with the relevant position of the magnetization, as described below Eq.(7)].

Note that the well-known expressions are recovered for the extreme cases, that are the perfect Hall bar and the Corbino disk. For an ideal Hall bar, the load resistance is infinite, and this implies $\alpha = 0$. We thus see that Eq. (38) converges to Eq. (19) as $\alpha \to 0$.

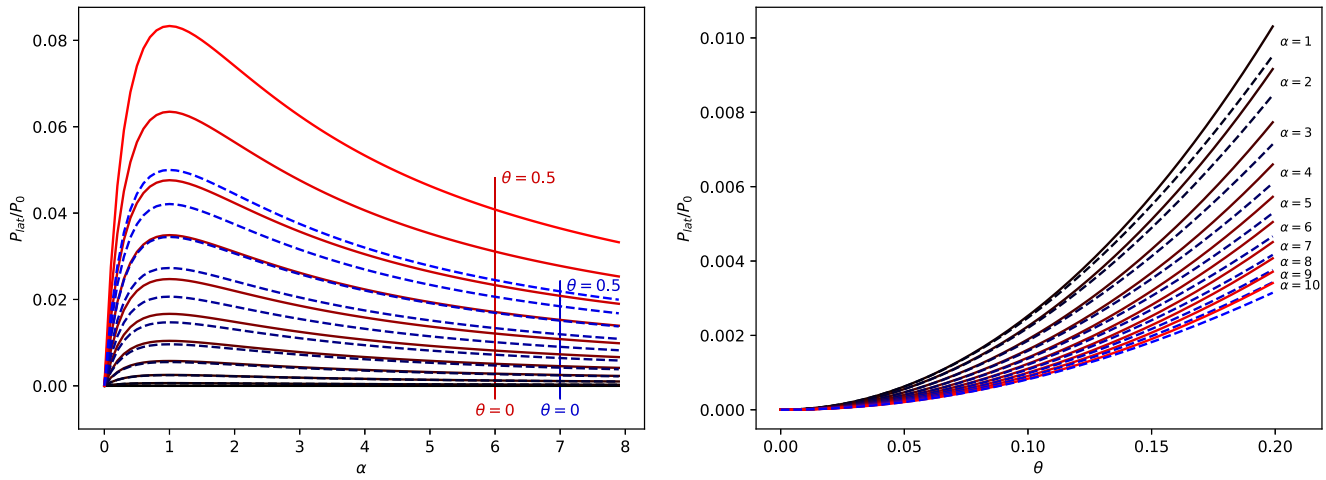

FIG. 2. Power efficiency $P_{\rm lat}/P_0$ for both AHE (red lines) and PHE (blue dashed line). Left: Efficiency as a function of the ratio $\alpha = R/R_\ell$ for values of Θ ranging from 0 to 0.5 with increments of 0.05. Right: Efficiency as a function of the Hall angle Θ.

Conversely, in a Corbino disk, we have $\alpha \to +\infty$ and the solutions converge to the well-known result

$$J_x^{\rm Cor} = \frac{n}{n_0} J_x^0 \quad \text{and} \quad J_y^{\rm Cor} = -\Theta J_x^0 \tag{39}$$

for both PHE and AHE.

We see that the second law of thermodynamics levels out the fundamental differences that define the two processes—PHE vs. AHE—at the microscopic scales.

B. Power injected in the load circuit

The total power $\tilde{P} = \tilde{P}_J + \tilde{P}_{\rm lat}$, given in Eq. (30), is the sum of the Joule heating $\tilde{P}_J$ dissipated inside the Hall device, and the power $\tilde{P}_{\rm lat}$ dissipated into the lateral passive circuit. Inserting the stationary state Eqs. (38) and using the first global condition in Eqs. (15) (assuming that $\delta n \ll n_0$, we have $\int_{-\ell}^{+\ell} \frac{dy}{n(y)} \simeq 2\ell/n_0$), the power dissipated in the lateral circuit reads

$$P_{\rm lat}^{\rm pl}(\alpha) \simeq \frac{2\ell S_{\rm lat}\left(J_x^0\right)^2}{\sigma_{pl}} \frac{\alpha}{(1+\alpha)^2} \Theta^2 \quad \text{and} \quad P_{\rm lat}^{\rm an}(\alpha) \simeq \frac{2\ell S_{\rm lat}\left(J_x^0\right)^2}{\sigma_{an}} \frac{\alpha}{(1+\alpha)^2} \Theta^2 \left(1 + 2\Theta^2 \alpha \left(\frac{n}{n_0} - 1\right)\right). \tag{40}$$

We define P_0, the power dissipated in the material in the absence of the Hall-like effect

$$P_0 \equiv P_J(\Theta = 0) = \frac{2\ell S_{\rm lat}\left(J_x^0\right)^2}{q\eta n_0} \tag{41}$$

The power P_0 can be retrieved experimentally by adjusting the magnetization according to Eq. (7). This leads to a very simple expression of the power efficiency due to the injection of the Hall current:

$$\frac{P_{\rm lat}^{\rm pl}}{P_0} \simeq \frac{\alpha}{(1+\alpha)^2} \frac{\Theta^2}{1-\Theta^2} \quad \text{and} \quad \begin{aligned} \frac{P_{\rm lat}^{\rm an}}{P_0} &\simeq \frac{\alpha}{(1+\alpha)^2} \frac{\Theta^2}{1+\Theta^2} \left(1 + 2\Theta^2 \alpha \left(\frac{n}{n_0} - 1\right)\right) \\ &\simeq \frac{\alpha}{(1+\alpha)^2} \frac{\Theta^2}{1+\Theta^2}. \end{aligned} \tag{42}$$

These results show that the power efficiencies for both effects are the same as a function of α, but their dependence on Θ differs. This behavior can be observed in Fig. 2, left panel, where this power is shown as a function of the variable α for several values of Θ, and in Fig. 2, right panel, where this power is shown as a function of the variable Θ for several values of α, for both AHE shown in red continuous lines and PHE shown in blue dashed lines. Specifically, both curves exhibit a unique maximum at the resistance-matching condition $\alpha = 1$ (i.e., $R = R_\ell$) where the resistances of the two subcircuits are equal. In other terms, the *maximum transfer theorem* holds true in both Hall-like systems. However, this result does not imply the validity of Kirchhoff's circuit law, as the stationary states in both cases are distinct whereas the lumped-element circuits for AHE and PHE appear identical (see Fig. 1).

Additionally, in typical materials, both anomalous Hall angles and planar Hall angles are relatively small, typically below 1%. As a result, the variation of the dissipated power between AHE and PHE with respect to the Hall angle is small but it can be observed experimentally. It is worth noting that

the discrepancy in dissipated power between the Hall bar and the Corbino disk also occurs at the second order in Θ. We observe however that if, instead of Eq. (41), we define the reference power as $P_0^{pl,an}(\alpha=0) = 2\ell S_{latt}\,(J_x^0)^2/\sigma_{pl,an}$ (i.e., the power of the perfect Hall bar for AHE and PHE separately), then we find no difference between the two power efficiencies in both cases.

C. Charge accumulation

In this last section we would like to compute the expression of the charge accumulation $\delta n(y)$ at the edges of a Hall bar contacted to the load circuit, whereas in Sec. III it was only done for a perfect Hall bar without load circuit.

We start with the solutions given by Eqs. (38), we rewrite $\vec{\nabla}\mu$ given by Eq. (10) as

$$\begin{cases} \partial_x\mu^{\rm pl} = -\dfrac{n_0}{n\sigma_{pl}}(J_x+\Theta J_y) \\ \partial_y\mu^{\rm pl} = -\dfrac{n_0}{n\sigma_{pl}}(\Theta J_x+J_y) \end{cases}, \qquad \begin{cases} \partial_x\mu^{\rm an} = -\dfrac{n_0}{n\sigma_{an}}(J_x-\Theta J_y) \\ \partial_y\mu^{\rm pl} = -\dfrac{n_0}{n\sigma_{an}}(\Theta J_x+J_y) \end{cases},$$

$$\text{and} \tag{43}$$

$$\begin{cases} \partial_x\mu^{\rm pl} = -\dfrac{J_x^0}{\sigma_{pl}}\left(1-\frac{n_0}{n}\frac{\alpha}{1+\alpha}\Theta^2\right) \\ \partial_y\mu^{\rm pl} = -\dfrac{J_x^0\Theta}{\sigma_{pl}}\left(1-\frac{n_0}{n}\frac{\alpha}{1+\alpha}\right) \end{cases}, \qquad \begin{cases} \partial_x\mu^{\rm an} = -\dfrac{J_x^0}{\sigma_{an}}\left(1+\Theta^2\frac{\alpha}{1+\alpha}\right) \\ \partial_y\mu^{\rm pl} = -\dfrac{J_x^0\Theta}{\sigma_{an}}\left(1+\Theta^2\frac{\alpha}{1+\alpha}-\frac{n_0}{n}\frac{\alpha}{1+\alpha}(1+\Theta^2)\right) \end{cases}.$$

We get

$$\begin{aligned} \nabla^2\mu^{\rm pl} &= -\frac{J_x^0\Theta}{\sigma_{pl}}\frac{\alpha}{1+\alpha}\frac{\partial_y(n/n_0)}{(n/n_0)^2} \\ &= -\frac{J_x^0}{qn_0\eta}\frac{\Theta}{1-\Theta^2}\frac{\alpha}{1+\alpha}\frac{\partial_y(n/n_0)}{(n/n_0)^2} \\ &= -\frac{q\lambda_D}{\varepsilon}n_{pl}\frac{\partial_y(n/n_0)}{(n/n_0)^2} \end{aligned} \qquad \text{and} \qquad \begin{aligned} \nabla^2\mu^{\rm an} &= -\frac{J_x^0\Theta(1+\Theta^2)}{\sigma_{an}}\frac{\alpha}{1+\alpha}\frac{\partial_y(n/n_0)}{(n/n_0)^2} \\ &= -\frac{J_x^0}{qn_0\eta}\Theta\frac{\alpha}{1+\alpha}\frac{\partial_y(n/n_0)}{(n/n_0)^2} \\ &= -\frac{q\lambda_D}{\varepsilon}n_{an}\frac{\partial_y(n/n_0)}{(n/n_0)^2}. \end{aligned} \tag{44}$$

The density of carriers reads

$$\begin{aligned} n_{pl} &= \frac{\varepsilon}{q\lambda_D}\frac{J_x^0}{qn_0\eta}\frac{\Theta}{1-\Theta^2}\frac{\alpha}{1+\alpha} \\ &= \nu\frac{\Theta}{1-\Theta^2}\frac{\alpha}{1+\alpha} \end{aligned} \qquad \text{and} \qquad \begin{aligned} n_{an} &= \frac{\varepsilon}{q\lambda_D}\frac{J_x^0}{qn_0\eta}\Theta\frac{\alpha}{1+\alpha} \\ &= \nu\,\Theta\frac{\alpha}{1+\alpha}, \end{aligned} \tag{45}$$

where we have set $\nu = \varepsilon J_x^0/(q^2\lambda_D n_0\eta)$. In this case, we find that the chemical potential is not harmonic (as was the case in Sec. III). The resulting formulation of Poisson's equation Eq. (2) is thus the same for both systems and is given by

$$-\lambda_D^2 n_0\nabla^2\ln\left(1+\frac{\delta n}{n_0}\right) - \lambda_D n_h\frac{\partial_y(\delta n/n_0)}{(n/n_0)^2} + \delta n = 0, \tag{46}$$

where we recall that the index h in n_h is given by $h = pl$ for the planar Hall case and by $h = an$ for the anomalous Hall case. We can linearize the equations in the regime $\delta n/n_0 \ll 1$ to get

$$-\lambda_D^2\partial_y^2\left(\frac{\delta n}{n_0}\right) - \frac{n_h}{n_0}\lambda_D\partial_y\left(\frac{\delta n}{n_0}\right) + \frac{\delta n}{n_0} = 0, \tag{47}$$

which can be solved exactly to give in both cases

$$\frac{q\lambda_D}{\varepsilon}\delta n(y) = e^{\frac{r_1 y}{\lambda_D}}\frac{E_{+\infty}e^{-\frac{r_2\ell}{\lambda_D}} - E_{-\infty}e^{\frac{r_2\ell}{\lambda_D}} + 2\,\mathrm{sh}\left(\frac{r_2\ell}{\lambda_D}\right)\frac{J_x^0\Theta}{\sigma_{pl}(1+\alpha)}}{2r_1\,\mathrm{sh}\left((r_1-r_2)\frac{\ell}{\lambda_D}\right)} + e^{\frac{r_2 y}{\lambda_D}}\frac{E_{+\infty}e^{-\frac{r_1\ell}{\lambda_D}} - E_{-\infty}e^{\frac{r_1\ell}{\lambda_D}} + 2\,\mathrm{sh}\left(\frac{r_1\ell}{\lambda_D}\right)\frac{J_x^0\Theta}{\sigma_{pl}(1+\alpha)}}{2r_2\,\mathrm{sh}\left((r_2-r_1)\frac{\ell}{\lambda_D}\right)}, \tag{48}$$

with

$$\begin{aligned} r_1^{\rm pl} &= \frac{1}{2}\left(-\frac{\nu}{n_0}\frac{\Theta}{1-\Theta^2}\frac{\alpha}{1+\alpha} - \sqrt{\left(\frac{\nu}{n_0}\frac{\Theta}{1-\Theta^2}\frac{\alpha}{1+\alpha}\right)^2+4}\right), \\ r_2^{\rm pl} &= \frac{1}{2}\left(-\frac{\nu}{n_0}\frac{\Theta}{1-\Theta^2}\frac{\alpha}{1+\alpha} + \sqrt{\left(\frac{\nu}{n_0}\frac{\Theta}{1-\Theta^2}\frac{\alpha}{1+\alpha}\right)^2+4}\right), \end{aligned} \qquad \text{and} \qquad \begin{aligned} r_1^{\rm an} &= \frac{1}{2}\left(-\frac{\nu}{n_0}\Theta\frac{\alpha}{1+\alpha} - \sqrt{\left(\frac{\nu}{n_0}\Theta\frac{\alpha}{1+\alpha}\right)^2+4}\right), \\ r_2^{\rm an} &= \frac{1}{2}\left(-\frac{\nu}{n_0}\Theta\frac{\alpha}{1+\alpha} + \sqrt{\left(\frac{\nu}{n_0}\Theta\frac{\alpha}{1+\alpha}\right)^2+4}\right). \end{aligned} \tag{49}$$

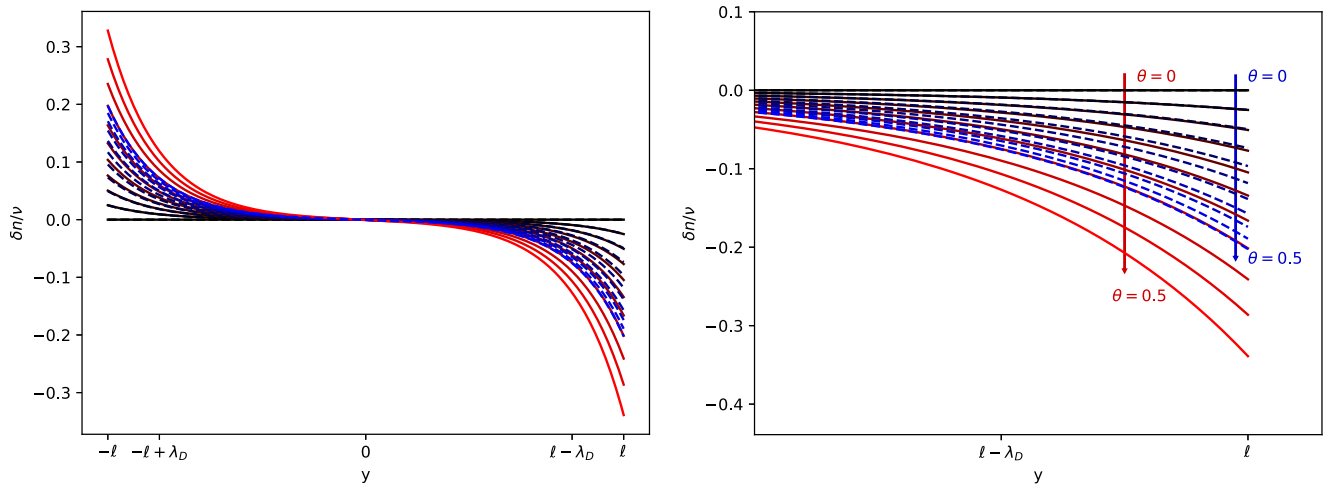

FIG. 3. The profiles of the charge accumulations $\delta n(y)/\nu$ for both AHE (blue) and PHA (red) for different values of the Hall angle Θ at the maximum $\alpha = 1$ (i.e., $R = R_\ell$) and for $\nu = 0.1 n_0$. Left: over the whole sample. Right: close to the right boundary. In both panels, the angle Θ ranges from 0 to 0.5 by increments of 0.05.

Without other external source of electric fields, we have

$$\frac{\delta n}{n_0}(y) = \frac{\nu}{n_0}\frac{\Theta}{1 \pm \Theta^2}\frac{1}{1+\alpha}\frac{1}{\mathrm{sh}\left((r_2 - r_1)\frac{\ell}{\lambda_D}\right)}\left(\mathrm{sh}\left(\frac{r_1 \ell}{\lambda_D}\right)\frac{e^{\frac{r_2 y}{\lambda_D}}}{r_2} - \mathrm{sh}\left(\frac{r_2 \ell}{\lambda_D}\right)\frac{e^{\frac{r_1 y}{\lambda_D}}}{r_1}\right), \tag{50}$$

which, in the limit $\alpha \to 0$, adequately gives us back the distribution of Eq. (27). The profiles of the charge accumulations $n(y)$ are functions of the parameters λ_D/ℓ, ν, α, and Θ. Despite the complexity of the expressions Eqs. (49) and Eqs. (50), the only difference between PHE and AHE is due to the difference as a function of Θ (see Fig. 3). We can see that changing the value of the Hall angle Θ will only change the amplitude of the distribution.

VI. CONCLUSION

We have investigated the properties of the injection of Hall currents into a lateral load circuit (Fig. 1) for both the planar Hall effect (PHE) and the anomalous Hall effect (AHE) with all other parameters being equal. The analysis is based on the principle of minimum power dissipation under the global constraints imposed to the system, and taking into account the screening effect. We derived analytical expressions of the distribution of charge carriers and currents for arbitrary values of the load resistance and Hall angle, focusing on the first order in the charge accumulation $\delta n/n_0$. Notably, our analysis recovers well-known limiting cases, such as the perfect Hall bar (infinite-load resistance) and the Corbino disk (zero-load resistance).

Despite the fundamental difference between the two effects at the microscopic scales, primarily characterized by time-reversal symmetry breaking, the accumulation of charge carriers, the distribution of currents, and the power efficiency of the injected Hall currents are surprisingly similar for both AHE and PHE [after having fixed the direction of the magnetization $\vec{m}$, according to Eqs. (7)]. The difference is then due to the Hall-angle dependence of the conductivities [Eq. (11)], i.e., observable at the second order in Θ (the maximum values of Θ are of the order of 1% in ordinary materials). In the case of the power efficiency, both curves have a maximum that corresponds to the resistance matching between the load circuit and the Hall bar. In other terms, *the maximum transfer theorem* is satisfied for both AHE and PHE. This property is not trivial because the system (shown in Fig. 1) cannot be simplified into a basic lumped-element circuit. These results showcase the relevance of the second law of thermodynamics for dissipative transport phenomena, which is found to level out the microscopic specificities and to invalidate the prediction of dissipationless transport for macroscopic Hall-like systems.

We mention the fact that the results obtained remain valid regardless of the mechanisms underlying both AHE and PHE, whether attributed to spin-orbit scattering, or to the topological properties of the band structure (Berry connection), as long as they give rise to a unique effective magnetic field. However, the approach followed in this analysis has its primary limitations in the quasiclassical approach and the local equilibrium hypothesis, so that the quantum anomalous Hall effect or the unconventional anomalous Hall effect may be beyond the limits of this model's validity. Nonetheless, the distinct characteristics of nanoscopic or quantum phenomena can now be easily identified and computed, thus allowing for a comparison between these unconventional systems and the conventional ones described in this study.

[1] S. Carnot, *Réflexion sur la puissance motrice du feu et sur les machines propres à développer cette puissance*, Bachelier Libraire, Paris 1824 and S. Carnot and R. Fox: *Reflexions on the Motive Power of Fire: A Critical Edition with the Surviving Scientific Manuscripts* (Manchester University Press, 1986).

[2] E. H. Hall, On a new action of the magnet on electric currents, Am. J. Math. **2**, 287 (1879).

[3] L. Onsager, Reciprocal relations in irreversible processes I, Phys. Rev. **37**, 405 (1931).

[4] L. Onsager, Reciprocal relations in irreversible processes II, Phys. Rev. **38**, 2265 (1931).

[5] The Nobel Prize in Chemistry 1968 was awarded to Lars Onsager "for the discovery of the reciprocal relations bearing his name, which are fundamental for the thermodynamics of irreversible processes" https://www.nobelprize.org/prizes/chemistry/1968/summary/.

[6] R. Karplus and J. M. Luttinger, Hall effect in ferromagnetics, Phys. Rev. **95**, 1154 (1954).

[7] J. Kondo, Anomalous Hall effect and magnetoresistance of ferromagnetic metals, Prog. Theor. Phys. **27**, 772 (1962).

[8] L. Berger, Side-jump mechanism for the Hall effect in ferromagnets Phys. Rev. B **2**, 4559 (1970).

[9] P. Nozières and C. Lewiner, A simple theory of the anomalous Hall effect in semiconductors, J. Phys. France **34**, 901 (1973).

[10] A. Crepieux and P. Bruno, Theory of anomalous Hall effect from the Kubo formula and the Dirac equation, Phys. Rev. B **64**, 014416 (2001).

[11] F. D. M. Haldane, Berry curvature on the fermi surface: Anomalous Hall effect as a topological fermi-liquid property, Phys. Rev. Lett. **93**, 206602 (2004).

[12] N. Nagaosa, J. Sinova, S. Onoda, A. H. MacDonald, and N. P. Ong, Anomalous Hall effect, Rev. Mod. Phys. **82**, 1539 (2010).

[13] T. Jungwirth, *et al.*, Spin-dependent phenomena and device concepts explored in (Ga, Mn)As, Rev. Mod. Phys. **86**, 855 (2014).

[14] H. Grimmer, General relations for transport properties in magnetically ordered crystals, Acta Cryst. A **49**, 763 (1993).

[15] G. Benenti, G. Casati, and R. S. Whilney, Fundamental aspects of steady-state conversion of heat to work at the nanoscale, Phys. Rep. **694**, 1 (2017).

[16] L. Smerjkal, J. Sinova, and T. Jungwirth, Emerging research landscape of altermagnetism, Phys. Rev. X **12**, 040501 (2022).

[17] I. Mazin, Altermagnetism then and now, Physics **17**, 4 (2024).

[18] C. Goldberg and R. E. Davis, New galvanomagnetic effect, Phys. Rev. **94**, 1121 (1954).

[19] A. Elzwawy *et al.*, Current trends in planar Hall effect sensors: Evolution, optimization, and applications, J. Phys. D: Appl. Phys. **54**, 353002 (2021).

[20] A. Schuhl, F. Nguyen Van Dau and J. R. Childress, Low-field magnetic sensors based on the planar Hall effect, Appl. Phys. Lett. **66**, 2751 (1995).

[21] M. I. Dyakonov and V. I. Perel, Possibility of orienting electron spins with current, Sov. Phys. JETP Lett. **13**, 467 (1971).

[22] M. Onoda, S. Murakami, and N. Nagaosa, Hall effect of light, Phys. Rev. Lett. **93**, 083901 (2004).

[23] C. Safranski, E. A. Montoya, and I. N. Krivorotov, Spin-orbit torque driven by a planar Hall current, Nat. Nanotechnol. **14**, 27 (2019).

[24] O. Shao *et al.*, Roadmap of spin orbit torques, IEEE Trans. Magn. **57**, 1 (2021),.

[25] R. Benda, J.M. Rubi, E. Olive, and J.E. Wegrowe, Towards Joule heating optimization in Hall devices, Phys. Rev. B **98**, 085417 (2018).

[26] M. Creff, F. Faisant, M. Rubì, and J.-E. Wegrowe, Surface current in Hall devices, J. Appl. Phys. **128**, 054501 (2020).

[27] P.-M. Déjardin and J.-E. Wegrowe, Stochastic description of the stationary Hall effect, J. Appl. Phys. **128**, 184504 (2020).

[28] F. Faisant, M. Creff, and J.-E. Wegrowe, The physical properties of the Hall current, J. Appl. Phys. **129**, 144501 (2021).

[29] M. Creff, E. Olive, and J.-E. Wegrowe, Screening effect in spin-Hall devices, Phys. Rev. B **105**, 174419 (2022).

[30] The system is a quadripole in contact with the electric generator and a load resistance. It is always possible to reduce the system composed of the generator and the Hall bar into a Thevenin equivalent circuit, but it is easy to show that the Thevenin resistance would then depend on the load resistance, which is in contradiction with the definition of an equivalent resistance.

[31] G. Viola and D. P. DiVincenzo, Hall effect gyrators and circulators, Phys. Rev. X **4**, 021019 (2014).

[32] D. Lacour, M. Hehn, M. Xu, and J.-E. Wegrowe, Injection of anomalous-Hall current into a load circuit, J. Appl. Phys. **135**, 193903 (2024).

[33] See the sections *relaxation phenomena* and *internal degrees of freedom* in Chapter 10 of S. R. De Groot, P. Mazur, *Non-equilibrium Thermodynamics* (North-Holland, Amsterdam, The Netherlands, 1962).

[34] D. Reguera, J. M. G. Vilar, and J. M. Rubì, The mesoscopic dynamics of thermodynamic systems, J. Phys. Chem. B **109**, 21502 (2005).

[35] For a degenerate metal, the expression is valid with $T = T^*$ at the first order in $\delta n/n_0$.

[36] F. Seitz, Note on the theory of resistance of a cubic semiconductor in a magnetic field, Phys. Rev. **79**, 372 (1950).

[37] T. McGuire and R. Potter, Anisotropic magnetoresistance in ferromagnetic 3D alloys, IEEE Trans. Magn. **11**, 1018 (1975).

[38] J.-E. Wegrowe, D. Lacour, H.-J. Drouhin, Anisotropic magnetothermal transport and spin Seebeck effect, Phys. Rev. B **89**, 094409 (2014).

[39] B. Madon, J.E. Wegrowe, M. Hehn, F. Montaigne, D. Lacour, and J.-E. Wegrowe, Corbino magnetoresistance in ferromagnetic layers : Two representative examples $Ni_{81}Fe_{19}$ and $Co_{83}Gd_{17}$ Phys. Rev. B **98**, 220405(R) (2018).

[40] L. Onsager and S. Machlup, Fluctuations and irreversible processes, Phys. Rev. **91**, 1505 (1953).

[41] S. Bruers, C. Maes, K. Netocný, On the validity of entropy production principles for linear electrical circuits, J. Stat. Phys. **129**, 725 (2007).

[42] L. Bertini, A. De Sole, D. Gabrielli, G. Jona-Lasinio, and C. Landim, Minimum dissipation principle in stationary non-equilibrium states, J. Stat. Phys. **116**, 831 (2004).